A comparison of the structure and dynamics of Global atmospheric oscillation in reality and in the CMIP5 climate models

I V Serykh

Shirshov Institute of Oceanology, Russian Academy of Sciences,
36, Nahimovskiy prospekt, Moscow, Russia, 117997

E-mail: iserykh@ocean.ru

Abstract. In this paper, global fields of mean anomalies of the sea-level atmospheric pressure and the surface air temperature are constructed for positive and negative phases of a recently discovered by Russian scientists Global atmospheric oscillation (GAO) with El Niño and La Niña as its elements. This is done using observations and their re-analyses, as well as the results of experiments with climate models. A GAO index is proposed, and its spectra, as well as spectra of El Niño – Southern Oscillation (ENSO), are calculated. It is shown that some of the modern models of ocean-atmosphere general circulation of the international Coupled Model Intercomparison Project Phase 5 (CMIP5) reproduce well the GAO spatial structure. The model temporal energy spectra, however, differ from the real ones in the general variation of the energy spectra of interannual-decadal oscillations, as well as in the periods of specific peaks in this range. A comparison of CMIP5 experiments called Historical and piControl shows that the climate models with the 11-year solar activity cycle forcing reproduce the GAO periodicity more accurately. It is concluded that the differences between the model spectra and the real ones cause major errors in the predictions of the El Niño onset for more than half a year.

1. Introduction

El Niño – Southern Oscillation (ENSO) is a well-known phenomenon observed in the ocean-atmosphere system. ENSO develops in a narrow equatorial Pacific Ocean band. That is, formally it is a regional event. However, it is commonly accepted that ENSO affects the meteorological processes on interannual to decadal time scales on the Earth. Numerous publications in Russian and other languages (see, for instance, [1, 2, 3]) are devoted to this problem. Note that a dozen of papers annually consider the importance of global influence of ENSO.

Some years ago a team of researchers from the Shirshov Institute of Oceanology RAS [4] suggested that there exists a Global atmospheric oscillation (GAO) with El Niño and La Niña developing at its extreme phases. In other words, they proposed that there is a primary interaction of some hydrometeorological processes taking place on the Earth, and ENSO is a major manifestation of these processes.

To detect the GAO, the global sea-level atmospheric pressure (SLP) fields corresponding to the ten strongest El Niño and La Niña events that took place in 1950-2010 were compared. They were used as a basis for constructing a mean field of differences between the El Niño and La Niña SLP fields. A major peculiarity of the mean field of differences was the presence of a wide positive SLP region

stretching in the zonal direction along the equator from Indonesia through the Indian Ocean, Africa, and the Atlantic to the Brazil coast. In the meridional direction this region is bounded by the 30° north and south latitudes. This region is surrounded on all sides by narrow bands of negative SLP differences. They merge and enhance in magnitude at the center and the eastern part of the Pacific Ocean crossing in the canonical zone of El Niño and La Niña development. Near the polar zones of the both hemispheres the SLP differences become positive again. To the south-west of South America there is a most pronounced area of positive SLP values. Here some researchers [5, 6] had discovered a high-power anticyclone developing simultaneously with El Niño.

Since the number of El Niño and La Niña events used to construct the mean field of differences by [4] was not large, it was not clear whether the mean field of SLP differences was statistically significant and, hence, whether the GAO was real. Therefore, in [7] the mean global field of SLP differences between the El Niño and La Niña events was recalculated with a larger number (23 and 25) of events that took place in 1920-2012. It is important that the global fields of root-mean-square SLP deviations from the mean fields of El Niño and La Niña were calculated separately for both groups of events. With these root-mean-square deviations, Student's t-test values were calculated for each geographical grid node. These values showed that the areas of positive and negative SLP differences in the GAO spatial structure are statistically highly significant (95% and even more). This proved that the GAO really exists.

This brings up the question, whether the modern coupled models of the ocean-atmosphere general circulation, that can simulate well many features of interannual variability in the Pacific Ocean tropics [8], can simulate the GAO. A comparison of the temporal energy spectra of the ENSO indices calculated with the observational data and the spectra obtained with the climate models of Coupled Model Intercomparison Project Phase 5 (CMIP5) has revealed a large scatter in the results [9, 10, 11, 12, 13]. The global and regional structures of anomalies of hydrometeorological fields at the El Niño events obtained with the CMIP5 models have also shown a wide spread in the observed anomalies [14, 15, 16, 17].

In the present paper, the global structures of SLP and the surface air temperature (SAT) differences between the El Niño and La Niña events, that is, between the positive and negative GAO phases, as well as the temporal energy spectra of the ENSO and GAO indices calculated with the observations and their re-analyses, are compared with the corresponding characteristics obtained by calculating the CMIP5 models in order to reveal possible shortcomings of the modern climate models.

2. Materials and methods of the study

The global monthly mean SLP fields used in the analysis were taken from the following sources: NCEP/NCAR Reanalysis on a 2.5°x2.5° grid over 1948-2014 [18], Met Office Hadley Center HadSLP2 on a 5°x5° grid over 1850-2014 [19], NOAA-CIRES 20th Century Global Reanalysis Version 2c on a 2°x2° grid over 1851-2011 [20], ECMWF ERA-20C on a 1°x1° grid over 1900-2010 [21], and JMA JRA-55 on a 1.25°x1.25° grid over 1958-2013 [22].

The global monthly mean values of sea surface temperature (SST) were taken from the following sources: Met Office Hadley Center HadISST on a 1°x1° grid over 1870-2014 [23], JMA COBE SST2 on a 1°x1° grid over 1850-2014 [24], and NOAA ERSST V4 on a 2°x2° grid over 1854-2015 [25, 26]. The global monthly mean data of the near-surface temperature of Met Office Hadley Center HadCRUT.4.4 on a 5°x5° grid over 1850-2014 [27] and the global monthly mean data of SAT from the above-mentioned re-analyses (NCEP/NCAR, 20thC_ReanV2c, ERA-20C and JRA-55) have also been analyzed.

For each of the above data sets at each grid node, the average annual variation in the corresponding time period was calculated, and then subtracted from the initial data. The thus obtained anomaly fields were used to calculate three indices: first, an El Niño index called the Extended Oceanic Nino Index (EONI). It is the mean SST anomaly over (5°S-5°N, 170°-80°W). There are typically more shipborne SST observations in this region than in the region (5°S-5°N, 170°-120°W) used to estimate a Niño 3.4 index that is the standard for determining El Niño. Second, the Equatorial Southern Oscillation Index

(ESOI) determined by the difference of the mean SLP anomalies between the regions of (5°S-5°N, 90°-140°E) and (5°S-5°N, 130°-80°W). Third, the Global Atmospheric Oscillation Index (GAOI), which is the next combination of normalized mean SLP anomalies over 10 areas of the maximal statistical significance of the differences between El Niño and La Niña related SLP-distributions [7]: (5°S-5°N, 35°-25°W) + (5°S-5°N, 55°-65°E) + (55°-65°N, 95°-85°W) + (65°-55°S, 95°-85°W) + (5°S-5°N, 145°-155°E) – (45°-55°N, 175°-165°W) – (45°-55°N, 15°-5°W) – (55°-45°S, 15°-5°W) – (55°-45°S, 175°-165°W) – (5°S-5°N, 95°-85°W). Unlike other ENSO and GAO indexes, GAOI contains the anomalies of the middle- and high-latitude regions, where the probability of GAO anomalies is large. Therefore, GAOI characterizes the whole planetary structure of the GAO, rather not only its tropical part. The GAOI varies synchronously with the EONI and ESOI, because its variations incorporate the Southern Oscillation. This shows that all atmospheric processes resulting in GAO evolve more or less synchronously. The linear trends in the thus obtained series of all the indices were removed by the least squares method to suppress the interdecadal climate changes.

El Niño and La Niña events were determined using EONI as follows: if this index within 5 successive months or longer exceeded +0.5°C, it was an El Niño, and if it was less than -0.5°C, it was a La Niña. The global fields of mean SLP and SAT anomalies were calculated for each event chosen in this way. These fields were averaged for El Niño and La Niña events separately. Then the difference between the thus obtained mean fields was calculated. The field of root-mean-square deviations of individual events from the mean field was determined for each type of events (El Niño and La Niña). This was used for estimating the fields of statistical significance of the differences between the mean fields according to Student's t-test with various probabilities. The positive and negative GAO phases were determined with GAOI, similarly to determining the El Niño and La Niña events. However, the root-mean-square deviation and the time in which the autocorrelation function of the GAOI reaches near-zero value served as a criterion for selection. For the GAO phases, global fields of mean SAT and SLP differences have also been constructed and the statistical significance of these anomalies has been estimated, which are very close to the fields obtained by EONI.

The temporal energy spectra of the indices were calculated using the fast Fourier transform (FFT). To provide maximum resolution of these spectra in the periods, a large group of spectra has been calculated. For this, the parts corresponding to the "windows" with widths ranging from the full length of the initial series to its half were taken, with the "windows" sliding along the entire length of the initial series. All thus obtained spectra were averaged, and the averaged spectrum was smoothed using a moving average [28].

The spectra of the so-called mappings of the indices on the annual time scale were calculated similarly. For this, a sequence of values of a month, for instance, the sequence of Januaries, Februaries, etc. was taken from the series under investigation. The "window" technique described above was used to calculate the spectrum for each sequence. Then all twelve spectra were averaged. This calculation method decreased the effect of the annual cycle on the estimation of the statistical significance of spectral density peaks, since the spectra of the mappings are not as "red" as those of typical continuous series. In fact, the range of periods under consideration in the spectra of mappings is limited to two years. However, this is sufficient for studying the GAO dynamics in 2- to 7-year periods, which are typical for El Niño.

The global fields of the mean amplitude of SLP and SAT oscillations during GAO and the energy spectra of the indices calculated using measurements and re-analyses were compared with the corresponding fields and spectra obtained similarly using the results of an experiment called Historical over 1850-2005 for the 47 coupled ocean-atmosphere general circulation models available in CMIP5: ACCESS1.0, ACCESS1-3, bcc-csm1-1, bcc-csm1-1-m, BNU-ESM, CanESM2, CCSM4, CESM1-BGC, CESM1-CAM5, CESM1-FASTCHEM, CESM1-WACCM, CMCC-CESM, CMCC-CM, CMCC-CMS, CNRM-CM5, CNRM-CM5-2, CSIRO-Mk3.6, EC-EARTH, FGOALS-s2, FIO-ESM, GFDL-CM2p1, GFDL-CM3, GFDL-ESM2G, GFDL-ESM2M, GISS-E2-H, GISS-E2-H-CC, GISS-E2-R, GISS-E2-R-CC, HadCM3, HadGEM2-AO, HadGEM2-CC, HadGEM2-ES, INM-CM4, IPSL-CM5A-LR, IPSL-CM5A-MR, IPSL-CM5B-LR, MIROC4h, MIROC5, MIROC-ESM, MIROC-ESM-

CHEM, MPI-ESM-LR, MPI-ESM-MR, MPI-ESM-P, MRI-CGCM3, MRI-ESM1, NorESM1-M, and NorESM1-ME [29]. A visual comparison of the obtained fields was performed. In addition, the differences between the fields after their linear interpolation to a 1°x1° grid were calculated. From the 47 CMIP5 models investigated, those that best reproduce the GAO global structure and the energy spectra of the indices were chosen. The method described above was used to calculate the fields and spectra obtained in an experiment called piControl for these climate models. This experiment, in contrast to Historical, has no external forcing of solar activity variations. The results of Historical and piControl experiments were compared to estimate the influence of external forces on the GAO and ENSO periodicity.

3. Discussion of the results

The comparison of the global fields of SLP and SAT differences between the GAO opposite phases constructed using observations and re-analyses has shown that they are very similar. Therefore, the present paper provides only for these fields an example of NOAA-CIRES 20th Century Reanalysis (figures 1a and 2a).

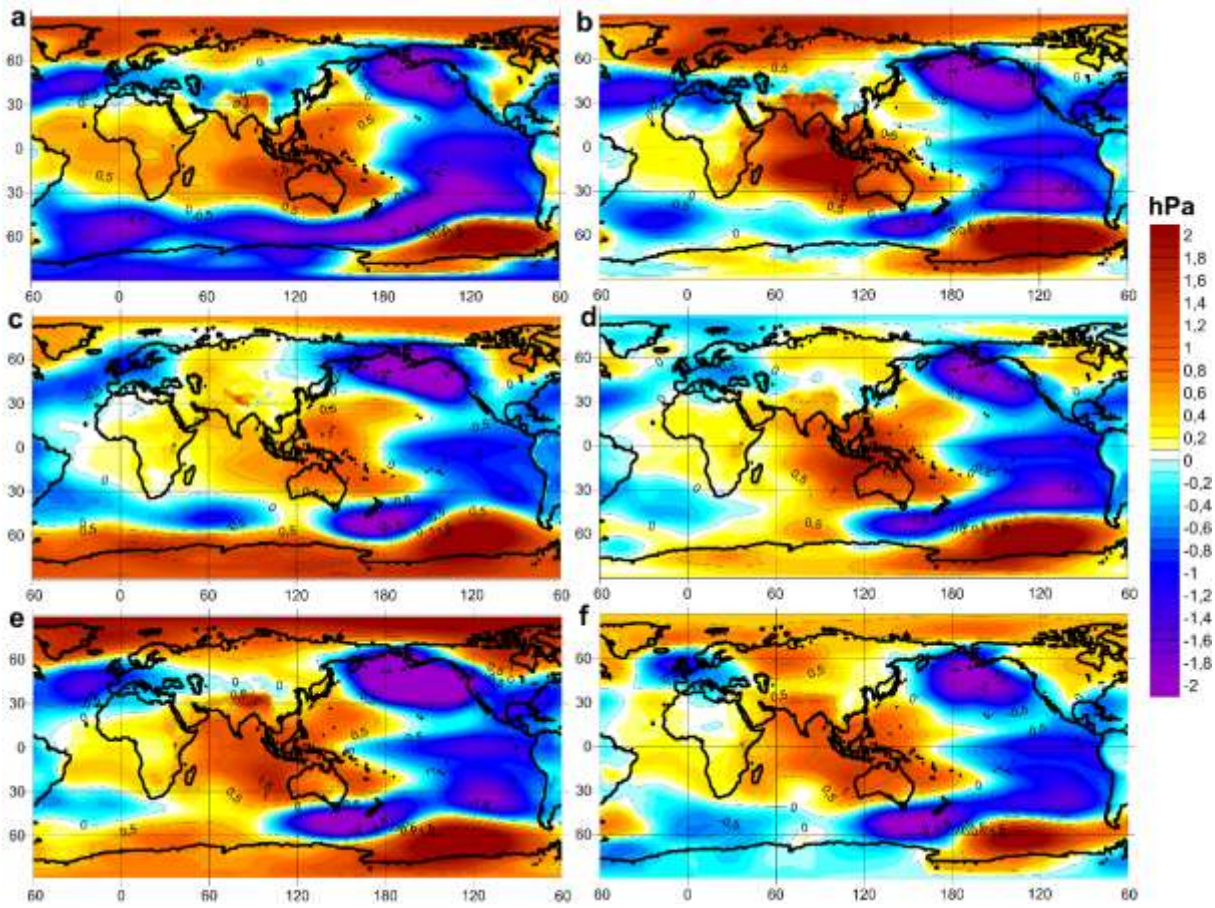

Figure 1. Fields of mean differences of sea-level pressure (SLP) between El Niño and La Niña events (positive and negative GAO phases) for NOAA-CIRES 20th Century Reanalysis v2c (a) and CMIP5 Historical experiment with climate models: CESM1-CAM5 (b), CMCC-CM (c), CNRM-CM5 (d), GFDL-CM3 (e) and HadGEM2-ES (f).

The SLP field of GAO (figure 1a) has a planetary structure with some symmetry about the equator and the meridian of 90°W, according to the location and relief of the continents. There is a wide zone of positive SLP GAO values in the tropics and subtropics of the Atlantic and Indian Oceans and the

western part of the Pacific Ocean surrounded by bands of negative values that intersect in the eastern part of the Pacific Ocean (120°-90°W) near the equator. Two zones of positive SLP anomalies are located almost symmetrically in high latitudes to the north and south of this intersection.

The above-described structure of the SLP oscillations caused by GAO is in good agreement with the accompanying SAT changes (figure 2a). They reveal a global structure of the temperature oscillations symmetric (with a correction for the continents) about the equator and the meridian passing through 120°W. There is a wide zone of positive SAT values in the tropics and subtropics of the Atlantic and Indian Oceans surrounded by bands of negative values. However, at their point of intersection in the central-eastern part of the Pacific Ocean tropics there is a "tongue" of positive SAT anomalies that is typical for El Niño. To the north and south of the "tongue", in high latitudes, there are two zones of positive values of SAT anomalies located almost symmetrically.

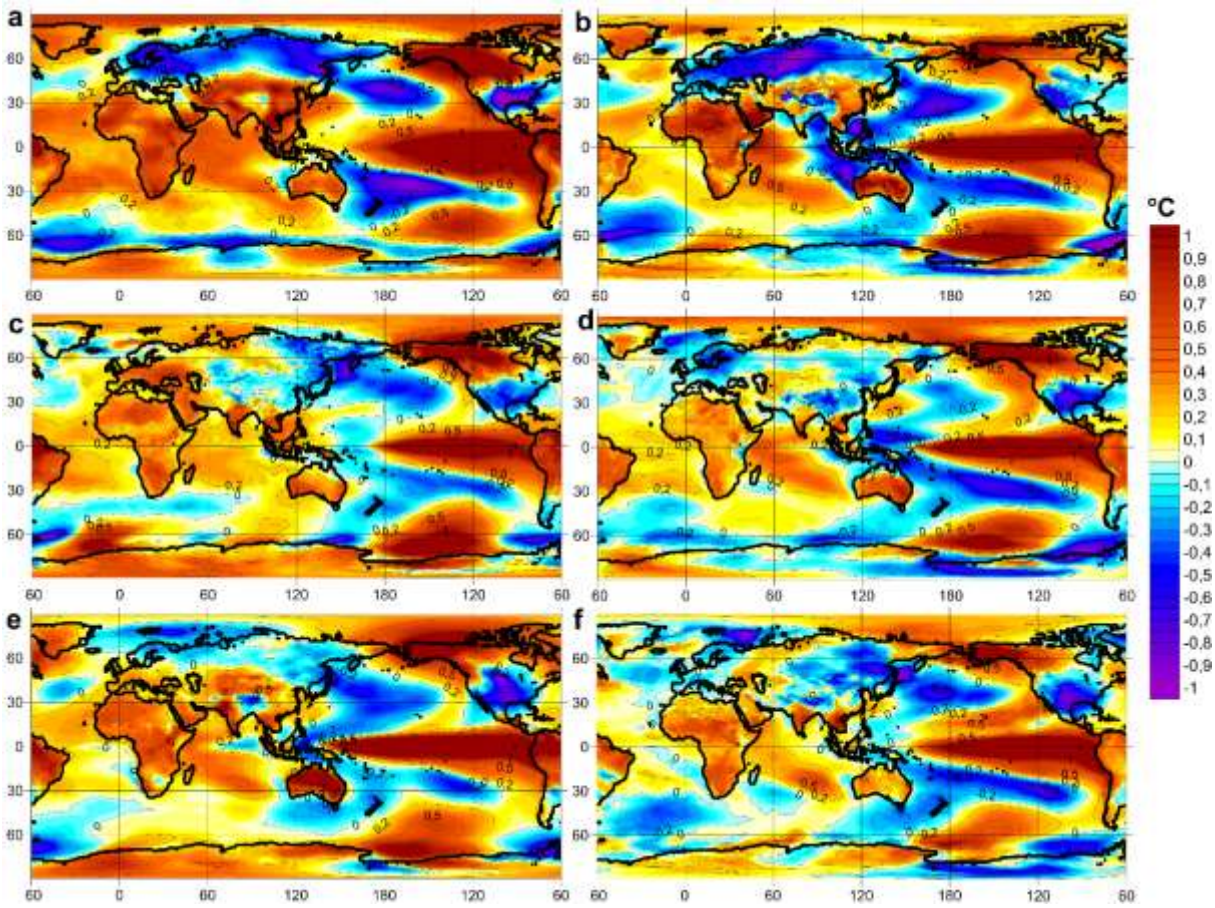

Figure 2. Fields of mean differences of surface air temperature (SAT) between El Niño and La Niña events (positive and negative GAO phases) for NOAA-CIRES 20th Century Reanalysis v2c (a) and CMIP5 Historical experiment with climate models: CESM1-CAM5 (b), CMCC-CM (c), CNRM-CM5 (d), GFDL-CM3 (e) and HadGEM2-ES (f).

The fields of SLP and SAT differences between the opposite GAO phases calculated with the results of the CMIP5 Historical experiment of climate models that are in the best agreement with the observations and their re-analyses are presented in figures 1b-1f and 2b-2f. In the SLP fields obtained by the models, the differences are underestimated (in comparison to the observations) in the tropics of the Atlantic Ocean and Africa (figure 1). This shows that in the models the teleconnections between the Indo-Pacific Walker circulation cells and the Atlantic and African ones are weaker. In the models results the bands of SLP negative values surrounding the wide tropical zone of positive values are not

clearly defined and have more breaks than the similar bands in the observations. This suggests that the interrelations between the tropics and mid-latitudes in the Hadley circulation are not fully taken into account in the models. In contrast to the observations, the SLP spatial structures obtained by the models better reproduce the corresponding SAT structures. Model's SLP spatial structures reveal the "tongue" of positive SST anomalies in the Pacific Ocean tropics typical for El Niño. This indicates that the effect of SST changes on SLP is overestimated in the models. In some models (not shown in figure 2) this SST "tongue" stretches too far to the western part of the Pacific Ocean covering the region of Indonesia, which results from the fact that equatorial upwelling in the central and western parts of the Pacific Ocean is overestimated in the models [8]. Note that the structure of SAT fields calculated by the models is less smooth over the continents than that of similar fields in the re-analyses. This indicates that the influence of relief in these models is overestimated.

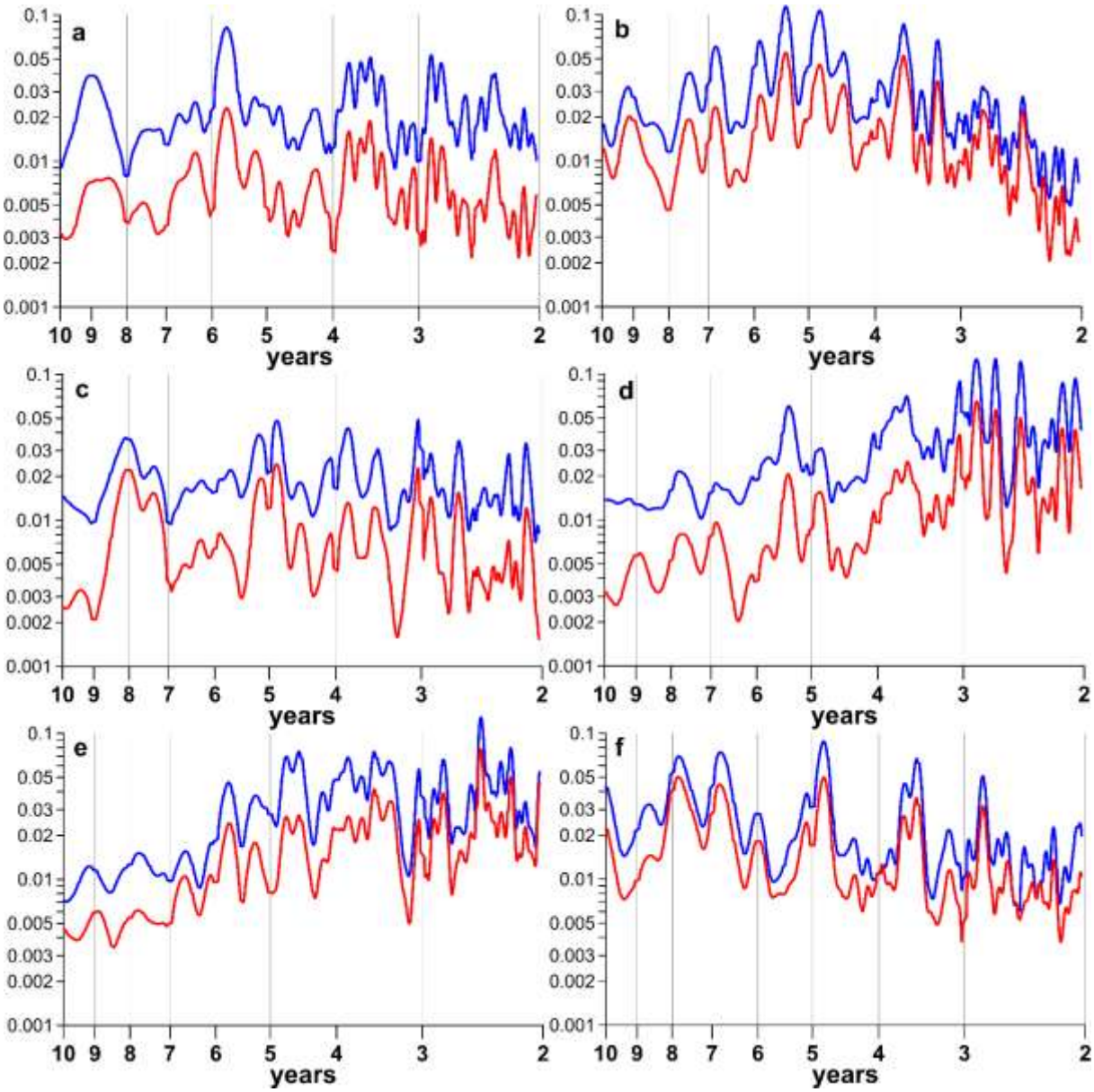

Figure 3. Energy spectra of EONI (red curves) and ESOI (blue curves) for NOAA-CIRES 20th Century Reanalysis v2c (a) and CMIP5 Historical experiment with climate models: CESM1-CAM5 (b), CMCC-CM (c), CNRM-CM5 (d), GFDL-CM3 (e) and HadGEM2-ES (f).

The best way to understand how the models reproduce ENSO and GAO temporal dynamics is to consider the observed and simulated temporal energy spectra of EONI and ESOI. In figure 3 these spectra are shown for the annual cycle mappings. These spectra allow more reliable estimation of the statistical significance of the spectral density peaks on scales from 2 to 10 years, since they are not as "red" as the spectra of their continuous analogs. It was found that the locations of peaks on the axis of the periods are very similar for all EONI, ESOI and GAOI spectra. This means that they can be analyzed simultaneously as one and the same spectrum.

Figure 3a shows that this real spectrum is practically "white", that is, its spectral density is the same if it is considered in a window of about a year or wider. From the model spectra presented, only the spectrum of the CMCC-CM model has this property (figure 3c). The spectra of two models, CESM1-CAM5 (figure 3b) and HadGEM2-ES (figure 3f), are "red". That is, the spectral density, in general, increases with the increasing period up to about 5-6 years. Then it does not increase, but even begins to slightly decrease. The spectral density of the CNRM-CM5 (figure 3d) and GFDL-CM3 (figure 3e) models, in general, decreases with the increasing period.

There are considerable differences between the real and model spectra also in the locations and powers of the spectral density peaks. It has long been accepted by most researchers that the major peaks in the ENSO spectra are statistically significant [30, 31]. This conclusion is very important, since some theoretical studies [32, 33, 34] of the periodically variable heat flux to the climate system from the Sun have shown that the appearance of peaks in the ENSO spectra in combinational harmonics of the annual period cannot be avoided.

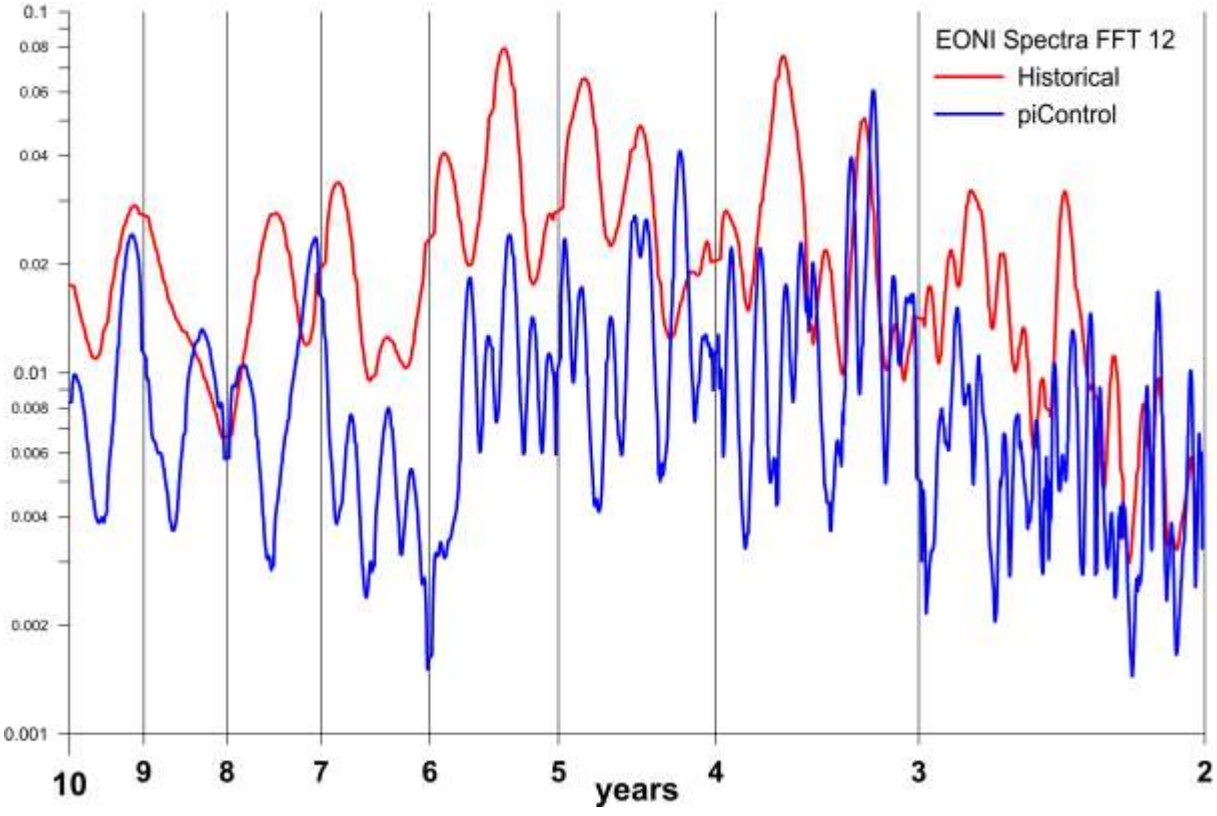

Figure 4. Energy spectra of normalized EONI of CESM1-CAM5 model in experiments Historical (red curve) and piControl (blue curve).

In the real spectrum (figure 3a) the major peaks are at periods of 5.6, 3.7 and 2.8 years. These are not combinational harmonics of the annual period. However, they can be considered as superharmonics 1:2, 1:3 and 1:4 of the 11-year solar activity cycle. This means that the climate system

responds to solar activity, although the energy of this action is very small. The response of the system to this small action is nonlinear. Therefore, it is evident not in the 11-year period itself, but on its superharmonics. This hypothesis has already been made [35].

The spectra of CMIP5 models shown in figure 3b-f were calculated using the results of the Historical experiment, which has 11-year solar cycle forcing. Therefore, some of the models, for instance, CESM1-CAM5 (figure 3b) and GFDL-CM3 (figure 3e), also have peaks in periods close to the above superharmonics. However, in the spectra calculated with the results of piControl experiment (without external forcing) these peaks are almost invisible in comparison to the other more powerful peaks (figure 4). Note also that the groups of powerful peaks in the real spectrum at periods of 2.4, 3.6 and 4.8 years can be considered as subharmonics 1:2, 1:3 and 1:4 of the Chandler wobble of Earth's poles with a period of about 1.2 years [36]. It was shown in [37] that this wobble can excite a warm surface current near the Pacific coast of Central America, that is, positive SST anomalies typical for El Niño. In the CMIP5 models the Chandler wobble is not taken into account. Therefore, such peaks are absent in most of the model spectra.

4. Conclusions

The comparison of the data of re-analyses and integrations of some modern climate models has shown that, on the whole, some of the coupled ocean-atmosphere general circulation models used in the international project CMIP5 reproduce well the planetary structures of anomalies in the sea-level atmospheric pressure (SLP) and surface air temperature (SAT) fields observed during El Niño and La Niña events. These planetary structures have been recently detected in the real atmosphere and called the Global atmospheric oscillation (GAO). There certainly exist numerous quantitative differences between the elements of the real and simulated GAO spatial structures.

An index, which is a combination of the mean SLP anomalies in 10 areas of the GAO global field, has been developed to characterize the GAO temporal dynamics. The temporal energy spectra of the GAO and ENSO indices on scales from 2 to 10 years have been estimated using observations and results of integrations of the CMIP5 models. These calculations have shown that there exist differences in the real and simulated spectra.

All the spectra, both the real and simulated ones, have many statistically significant peaks of spectral density. However, their location in the axis of the periods of the model spectra differs considerably from that of the real spectra. There are three major peaks in the real spectra for periods of 5.6, 3.7 and 2.8 years, that is, superharmonics of the 11-year solar activity cycle. From the model spectra presented, only two models have peaks for periods close to those for the above-mentioned periods if these spectra are calculated using the results of a Historical experiment in which the changes in solar activity is taken into account. If the spectra are calculated with the results of these models in the piControl experiment (without external 11-year solar activity cycle forcing), no peaks are observed on the above superharmonics. This is indirect evidence that the major peaks in the real spectra can be considered as nonlinear responses of the real climate system to the 11-year solar activity cycle.

The real spectra also have a sequence of peaks for periods of 2.4, 3.6 and 4.8 years which can be interpreted as subharmonics of the Chandler wobble of the Earth's poles, whose period is about 1.2 years. In none of the CMIP5 experiments the Chandler wobble was taken into account. Therefore, it is not surprising that the most of model spectra do not reproduce such peaks.

Taking into account the differences in reproducing the GAO spatial structure by the modern climate models and, especially, the temporal spectra of the GAO and ENSO indices, it is clear why the El Niño and La Niña events cannot be presently predicted for more than half a year. It seems that to overcome this so-called "spring predictability barrier" some periodic external forces on the climate system, such as the changes in solar activity and the Chandler wobble of the Earth's poles, should be taken into account.

Acknowledgments

This work was supported by the Russian Science Foundation (project no. 14-50-00095).

References

[1] Voskresenskaya E N, Polonsky A B 1993 Air pressure fluctuations in the North Atlantic and their relationship with El Nino - southern oscillations *Physical oceanography* **4** 275–82
[2] McPhaden M J, Zebiak S E, Glantz M H 2006 ENSO as an integrating concept in Earth science *Science* **314** 1740–45
[3] Peng J B, Chen L T, Zhang Q Y 2014 The relationship between the El Nino/La Nina cycle and the transition chains of four atmospheric oscillations. Part I: The four oscillations *Adv. Atmos. Sci.* **31** 2 468–79
[4] Byshev V I, Neiman V G, Romanov Yu A, Serykh I V 2012 El Niño as a consequence of the global oscillation in the dynamics of the Earth's climatic system *Doklady Earth Sciences* **446** (1) 1089–94
[5] Peterson R G, White W B 1998 Slow teleconnections linking the Antarctic Circumpolar Wave with the tropical El Nino – Southern Oscillation *J. geophys. Res.* **103** 24573–83
[6] Romanov Y A, Romanova N A, Romanov P Y 2008 Distribution of icebergs in the Atlantic and Indian ocean Sectors of the Antarctic region and its possible links with ENSO *Geophys. Res. Lett.* **35** LO2506
[7] Byshev V I, Neiman V G, Romanov Yu A, Serykh I V, Sonechkin D M 2016 Statistical significance and climatic role of the Global Atmospheric Oscillation *Oceanology* **56** (2) 165–71
[8] Volodin E M, Diansky N A 2004 El Nino in a coupled ocean-atmosphere general circulation model *Russian Meteorology and Hydrology* **12** 5–14
[9] Bellenger H, Guilyardi E, Leloup J, Lengaigne M, Vialard J 2014 ENSO representation in climate models: from CMIP3 to CMIP5 *Clim. Dyn.* **42** 1999–2018
[10] Privalsky V, Yushkov V 2015 ENSO influence upon global temperature in nature and in CMIP5 simulations *Atmos. Sci. Let.* **16** 240–45
[11] Rao J, Ren R C 2014 Statistical characteristics of ENSO events in CMIP5 models *Atmos. Oceanic Sci. Lett.* **7** 546–52
[12] Ren H L, Zuo J, Jin F F, Stuecker M F 2015 ENSO and annual cycle interaction: the combination mode representation in CMIP5 models *Clim. Dyn.* DOI 10.1007/s00382-015-2802-z
[13] Stevenson S L 2012 Significant changes to ENSO strength and impacts in the twenty-first century: Results from CMIP5 *Geophys. Res. Lett.* **39** L17703
[14] Hurwitz M M *et al* 2014 Extra-tropical atmospheric response to ENSO in the CMIP5 models *Clim. Dyn.* DOI 10.1007/s00382-014-2110-z
[15] Jha B, Hu Z, Kumar A 2014 SST and ENSO variability and change simulated in historical experiments of CMIP5 models *Clim. Dyn.* **42** 2113–24
[16] Oh J H, Shin D W, Cocke S D, Baigorria G A 2014 ENSO Teleconnection Pattern Changes over the Southeastern United States under a Climate Change Scenario in CMIP5 Models *Advances in Meteorology* **2014** 648197
[17] Weare B C 2013 El Nino teleconnections in CMIP5 models *Clim. Dyn.* **41** pp 2165–2177
[18] Kalnay E *et al* 1996 The NCEP / NCAR 40-year reanalysis project *Bull. Amer. Meteor. Soc.* **77** 437–71
[19] Allan R J, Ansell T J 2006 A new globally-complete monthly historical gridded mean sea level pressure data set (HadSLP2): 1850-2004 *J. Climate* **19** 5816–46
[20] Compo G P, Whitaker J S, Sardeshmukh P D et al 2011 The Twentieth Century Reanalysis Project *Quarterly J. Roy. Meteorol. Soc.* **137** 1–28
[21] Stickler A *et al* 2014 ERA-CLIM: Historical Surface and Upper-Air Data for Future Reanalyses *Bull. Amer. Meteor. Soc.* **95** (9) 1419–30
[22] Kobayashi S *et al* 2015 The JRA-55 Reanalysis: General Specifications and Basic Characteristics *J. Met. Soc. Jap.* **93** (1) 5–48
[23] Rayner N A *et al* 2003 Global analyses of sea surface temperature, sea ice, and night marine air

temperature since the late nineteenth century *J. Geophys. Res.* **108** (D14) 4407
[24] Hirahara S, Ishii M, Fukuda Y 2014 Centennial-scale sea surface temperature analysis and its uncertainty *J. of Climate* **27** 57–75
[25] Huang B *et al* 2015 Extended reconstructed sea surface temperature version 4 (ERSST.v4). Part I: Upgrades and intercomparisons *J. Clim.* **28** (3) 911–30
[26] Liu W *et al* 2015 Extended reconstructed sea surface temperature version 4 (ERSST.v4): Part II. Parametric and structural uncertainty estimations *J. Clim.* **28** (3) 931–51
[27] Jones P D, Lister D H, Osborn T J 2012 Hemispheric and large-scale land surface air temperature variations: An extensive revision and an update to 2010 *J. Geophys. Res.* **117** D05127
[28] Serykh I V, Sonechkin D M 2017 Manifestations of motions of the Earth's pole in the El Niño – Southern Oscillation rhythms *Doklady Earth Sciences* **472** (2) 256–59
[29] Taylor K E, Stouffer R J, Meehl G A 2012 Overview of CMIP5 and the experiment design *Bull. Am. Meteor. Soc.* **93** 485–98
[30] Trenberth K E 1976 Spatial and temporal variations of the Southern Oscillation *Quart. J. Roy. Meteor. Soc.* **102** 639–53
[31] Torrence C, Compo G P 1997 A practical guide to wavelet analysys *Bull. Amer. Meteorol. Soc.* **79** (1) 61–78
[32] Jin F F, Neelin J D, Ghil M 1994 El Nino on the devil's: annual subharmonic steps to chaos *Science* **264** 70–72
[33] Jin F F, Neelin J D, Ghil M 1996 El Nino/Southern Oscillation and the annual cycle: Subharmonic frequency locking and aperiodicity *Physica D.* **98** 442–65
[34] Tziperman E, Stone L, Cane M A et al 1994 El Nino chaos: overlapping of resonances between the seasonal cycle and the Pacific Ocean – atmosphere oscillator *Science* **264** 72–74
[35] Vakulenko N V, Sonechkin D M 2011 Evidence of the solar Activity's effect on El Nino Southern Oscillation *Oceanology* **51** (6) 935–39
[36] Sidorenkov N S 2009 *The interaction between Earth's rotation and geophysical processes* (Weinheim: Wiley-VCH & Co. KCaA) p 305
[37] Serykh I V, Sonechkin D M 2016 Confirmation of the oceanic pole tide influence on El Niño *Sovremennye Problemy Distantsionnogo Zondirovaniya Zemli iz Kosmosa* **13** (2) 44–52